Iraqi Journal of Science

ISSN: 0067-2904

Improving Reflectors Visualization by Implementing Surface-Consistent Deconvolution in 2D Seismic Data Related to the Western Region of Iraq

Zeyad H. Khalaf*, Ali M. Al-Rahim
Department of Geology, College of Science, University of Baghdad, Baghdad, Iraq

Received: 11/12/2024 Accepted: 17/3/2025 Published: 30/3/2026

Abstract

This study concentrates on the analysis of 2D seismic reflection surveying data obtained from a seismic line characterized by a considerable amount of noise and reverberations. The goal is to enhance data quality by employing the surface-consistent deconvolution technique, which encompasses two variations; gapped and spike deconvolution. The unique applications offered by utilizing the Global Claritas software to achieve optimal outcomes, which assist in the quality of seismic data analysis and interpretation. Several tests were carried out on the seismic data, revealing that the application of Spike deconvolution with an operator length of 220 milliseconds and a prediction lag of 2 milliseconds led to enhancements in the data. This process improved the wavelet continuity and reduced noise levels. Through the tests conducted on gapped deconvolution, it was determined that the optimal operator length for the data is 220 milliseconds, accompanied by a prediction delay of 20 milliseconds, which got excellent results in eliminating reverberations and improving the vertical resolution of the seismic. The deconvolution application technique was effective in reducing noise for shallow-depth data. According to the results extracted after applying Gapped deconvolution, it is regarded as the most effective method for the data pertaining to the western region, as well as offering a clearer image of the subsurface reflectors, this would increase the resolution of the seismic section in detecting reflection surfaces and to distinguish seismic attributes.

Keywords: Seismic section resolution, Surface-consistent deconvolution, Spike, Gapped, Western Region, Iraq

تحسين تصوير العواكس من خلال تنفيذ التلفلف المتوافق مع السطح في البيانات الزلزالية ثنائية الأبعاد المتعلقة بالمنطقة الغربية من العراق

زياد حيدر خلف* ، علي مكي حسين الرحيم
قسم علم الأرض، كلية العلوم، جامعة بغداد، بغداد، العراق

الخلاصة

تركزت هذه الدراسة على تحليل بيانات الزلازل ثنائية الأبعاد التي تم الحصول عليها من خط زلزالي يتميز بضوضاء وصدى كبيرين. الهدف هو تحسين جودة البيانات من خلال استخدام تقنية فك التلفلف المتسقة مع السطح، والتي تشمل نوعين: فك التداخل الفجوة وفك التداخل النبضي. تساعد التطبيقات الفريدة

*Email: zeyed.haidar2308@sc.uobaghdad.edu.iq

التي يتم تقديمها من خلال استخدام برنامج كلوبل كلارتاس لتحقيق نتائج مثالية في تحسين جودة تحليل البيانات الزلزالية وتفسيرها. تم إجراء عدة اختبارات على البيانات الزلزالية، مما كشف أن تطبيق إزالة التداخل النبضي مع طول مشغل يبلغ 220 مللي ثانية وتأخير تنبؤي يبلغ 2 مللي ثانية أدى إلى تحسينات في البيانات، من حيث تحسين استمرارية المويجات وتقليل مستويات الضوضاء. من خلال الاختبارات التي أجريت على فك التداخل الفجوي، تم تحديد أن الطول الأمثل للمشغل للبيانات هو 220 مللي ثانية، مصحوبًا بتأخير تنبؤي قدره 20 مللي ثانية، والذي حقق نتائج ممتازة في القضاء على الصدى زيادة الدقة العمودية في العواكس الموجودة في البيانات الزلزالية مع زيادة على استمرارية الموجات الزلزالية، كما أنه قلل بشكل كبير من الضوضاء في البيانات القريبة من السطح. ووفقًا للنتائج المستخرجة بعد تطبيق فك الالتواء الفجوي، يُنظر إليه على أنه الطريقة الأكثر فعالية للبيانات المتعلقة بالمنطقة الغربية، فضلاً عن تقديم صورة أكثر وضوحًا للعاكسات تحت السطحية، وهذا من شأنه أن يزيد من دقة المقطع الزلزالي في اكتشاف أسطح الانعكاس وتمييز السمات الزلزالية.

1. Introduction

Reflection seismic data processing is a sequence of methods used to transform the reflected raw seismic wave arrivals into subsurface images that can be used for geophysical and geological interpretation [1]. Seismic exploration aims to determine the location and size of underground oil and gas reserves and to reduce the risk of drilling dry wells [2]. The seismic reflection method depends on the generation of mechanical waves, with known frequencies that interface with the Earth's layers and are then reflected to a surface to be received by geophones [3]. Geophones record the reflected waves, which are then processed to create a complete model of the underlying subsurface structures [4]. The characteristics of rocks and their bearing capacities are essential factors that must be considered during geophysical surveys [5]. After the data is acquired from field surveying, data starts with the first stage of processing, which checks the data quality of shot-gathers and continues until the final stack, which composes the final subsurface image [6]. One of the most important steps in seismic processing is the deconvolution process, due to its ability to improve the signal-to-noise ratio and enhance data quality by reducing noise and reverberation as much as possible [7].

Deconvolution is the process that leads to uncoupling between the source wavelet and the reflectivity series in seismic data to obtain the most accurate information from the subsurface image [8]. There are many types of deconvolution techniques used in seismic processing. The surface-consistent deconvolution “SCDECON” is one of the important types that decomposes the wavelet signal into offset, receiver, source, and reflectivity series [9].

This study will use the Surface-Consistent Deconvolution “SCDECON” to process one 2D-seismic data line, which belongs to the western region of Iraq near Al-Qaim District in Anbar Governorate, as shown by the red rectangular in Figure-1B. The seismic line was implemented using vibration trucks, and the type of shooting is mid-shooting (Symmetrical). The length of the seismic line is 54.05 km, and the distance between each two receiving points or two source points is 50 meters. The seismic data is characterized by its noise and poor quality due to the nature and properties of the rock layers [10]. Hence, the use of surface-consistent deconvolution can enhance the data from the noise effects by its properties, such as preserving the amplitude balance and phase characteristics [11].

The contractor that supplied us with the seismic data chose to keep the details confidential by refraining from disclosing the exact location of the seismic line in the Western Desert of Iraq. The study aims to improve the temporal resolution of the seismic data on the shot-gathers before the stacking stage and attenuate the noise and reverberation on the recorded data.

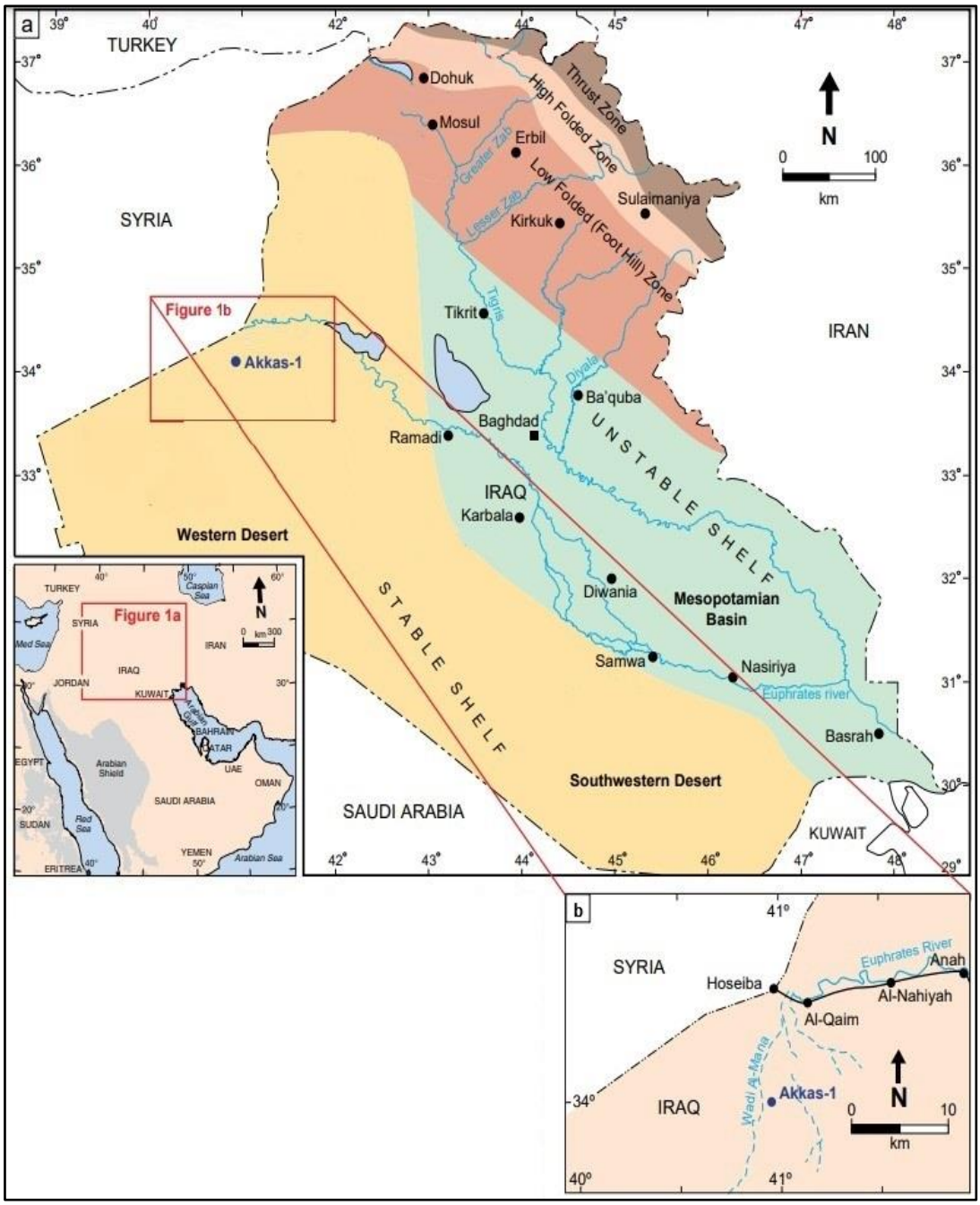

Figure 1: A- Shows the location of Iraq, which is related to other countries and the tectonic division of Iraq. B- represents the area near the seismic survey line [12].

Figure 2 explains the strata succession of Akkas-1 well. The well shows the lithological sequence during the Tertiary, Cretaceous, and Paleozoic periods for a wide range of formations extending to 2431 meters in depth. Through the general view of the well, it consists of several sedimentary cycles during the periods mentioned and found that the thickness of the formations in the Tertiary and Cretaceous periods is thin and of different lithologies and velocity, which consequently affects the quality of the seismic data and increases its reverberation of waves. In contrast, the thickness of the formations in the Paleozoic period is large and close in lithology.

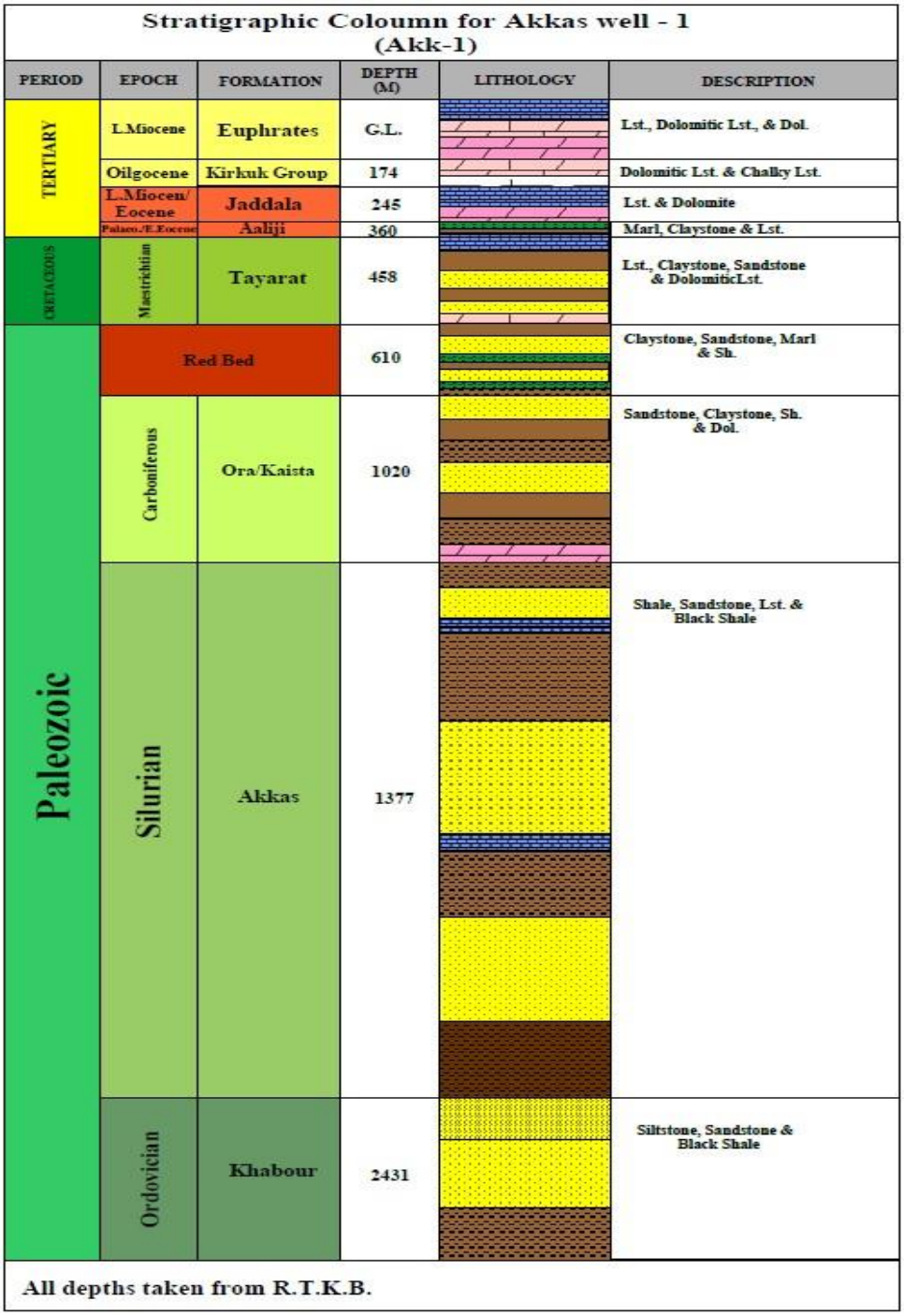

Figure 2: A general view of the succession of Akkas-1 well in the study area. Many sedimentary cycles are shown during the Tertiary, Cretaceous, and Paleozoic periods [13].

2. Theoretical background

The seismic techniques require the generation of Seismic or mechanical waves by selected source types like vibration trucks. These waves travel through the Earth's layer to convolve with boundaries and layer contacts. Then they are reflected to the surface to be received by detectors called geophones as shown in Figure 3 when the survey is implemented on the land [14]. The recorded seismic waves, which are received by geophones, are transferred as digital data and then converted to analog signals by some sequence of devices, which allows the data to be previewed as SEG-D files [15]. Standard seismic data format "SEG-D" file is converted to Seismic data exchange format "SEG-Y" to let the seismic processing software interpret

and analyze the data more effectively, enabling seismic processing programs to deal more easily with the acquired data [16]. Surface-consistent deconvolution techniques work to remove surface-related effects, including variations in source and receiver coupling and near-surface conditions, which can cause fluctuations in signals [17]. The underlying assumption is that these signal distortions are linked to surface factors and are consistent with the source and receiver positions, as shown in Equation 1 [18]. The different deconvolution algorithms are utilized for each component to account for local variations [19]. The non-stationary seismic data that exhibit spatially varying surface conditions, particularly from land seismic surveys, employing surface-consistent deconvolution proves to be quite beneficial [20].

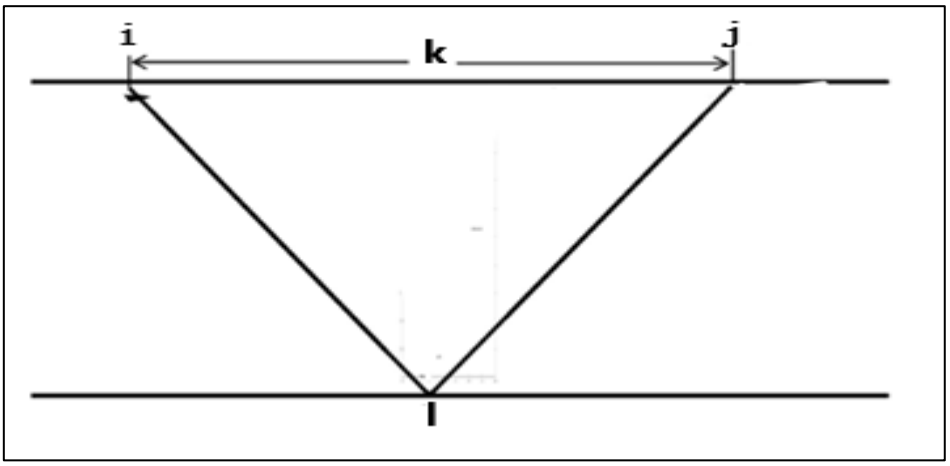

Figure 3*:* Surface consistent deconvolution model for the seismic trace.

$$d_{ij}(t) \approx \underbrace{S_i(t) * r_j(t)}_{\text{Near-surface}} * \underbrace{h_k(t) * y_l(t)}_{\text{Subsurface}} \quad (1)$$

Where the symbols in Equation (1) refer to the following [21]:

- (*): refers to the convolution process.
- $d_{ij}(t)$: The recorded seismic data at i^{th} is the seismic receiver traces, and j^{th} is the source number recorded.

✓ i: Coordinate of the seismic source.
✓ j: Coordinate of the receiver.

- $S_i(t)$: The source effect on the surface at the coordinate i.
- $r_j(t)$: The receiver effect on the surface at the coordinate j.
- $h_k(t)$: The offset effect at the offset coordinate k.

✓ k: Coordinate related to the subsurface impulse response.

- $y_l(t)$: The subsurface responses beneath surface location l.

✓ l: Coordinate related to the reflectivity.

3. Materials and Methods

The software used for the seismic processing was “Global Claritas”. This software is one of the commonly used programs. This program was developed by the New Zealand Institute of Geological and Nuclear Sciences [22].

SCDECON affects spatially-varying as a gapped deconvolution and time-varying as spiking deconvolution. The deconvolution is applied in two stages: Spiking SCDECON to select the best operator length, and the gapped SCDECON to find the best prediction lag.

To verify the precision of the deconvolution process, both spike and gapped methods employed an auto-correlogram and an amplitude spectrum graph [23]. This was done using the software "XVIEW" before and after the deconvolution process.

3.1 Spiking Surface-Consistent Deconvolution

The "SCDECON" software is used as the central surface-consistent deconvolution processor. This kind of deconvolution needs to provide the parameter of the operator length, prediction lag, and the Whiting noise percentage. The process was done by conducting six tests to find the best operator length, considering the sample rate as prediction lag, which is 2 ms for all tests, which is equal to the sample rate of the recording data, and using operator lengths ranging from 180 ms to 400 ms and fixed whiting noise percentage 0.01% according to (Table-1).

Table 1: Tests applied to find the best parameters for spiking SCDECON.

Test No.	Operator Length (ms)
1	180
2	200
3	220
4	260
5	300
6	400

Raw autocorrelated data is shown in Figure-1, and the results are shown in Figure-2 Post-deconvolution. To prove the result of the deconvoluted data, the amplitude spectrum graph was used as shown in Figure 3 before and after deconvolution, Figure 4. The Deconvolution-extracted data is transformed from the shot-gather domain into the CDP-gather domain. The normal-move-out correction is applied to prepare it for stacking, which is the last stack of the data. Using a bandpass filter to reduce the noise acquired from applying the deconvolution, the bandpass frequencies used are [11-13] Hz for the high-pass filter, and for the low-pass filter they are [45-50] Hz.

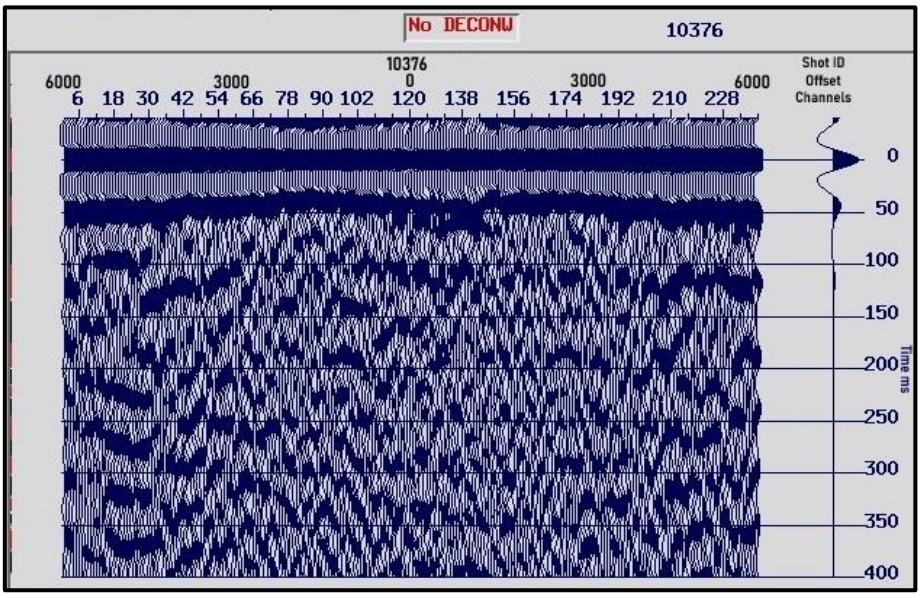

Figure 4: Raw data autocorrelation.

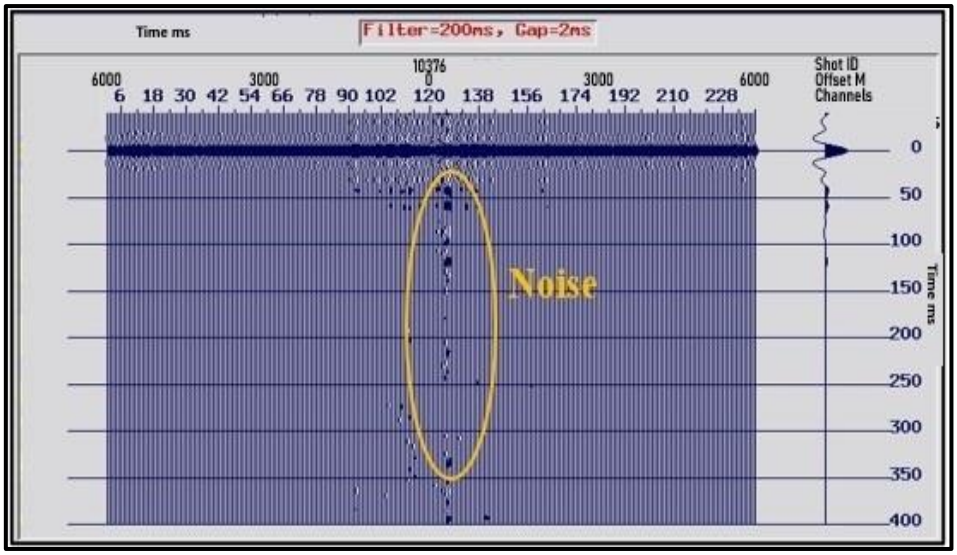

Figure 5: Autocorrelation after applying spiking SCDECON, operator length 220 ms, prediction lag 2ms.

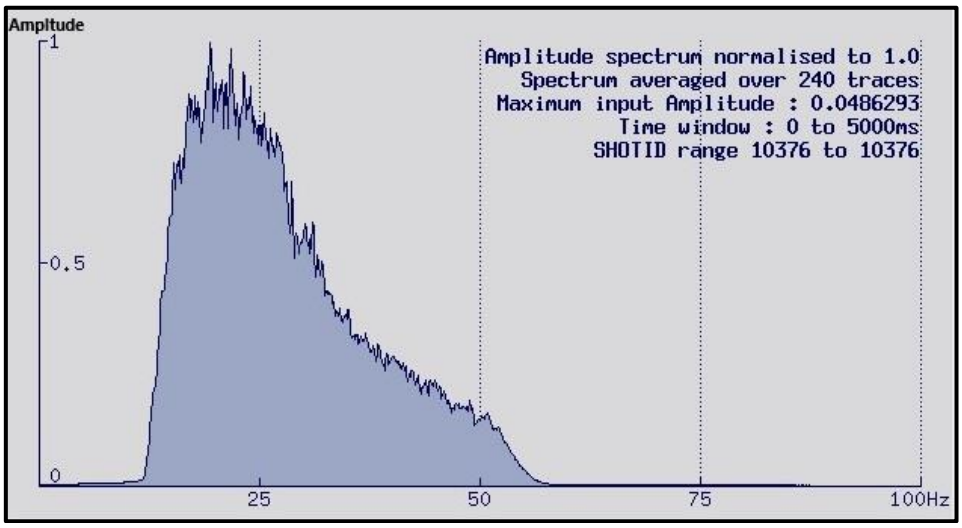

Figure 6: Amplitude Spectrum for raw data.

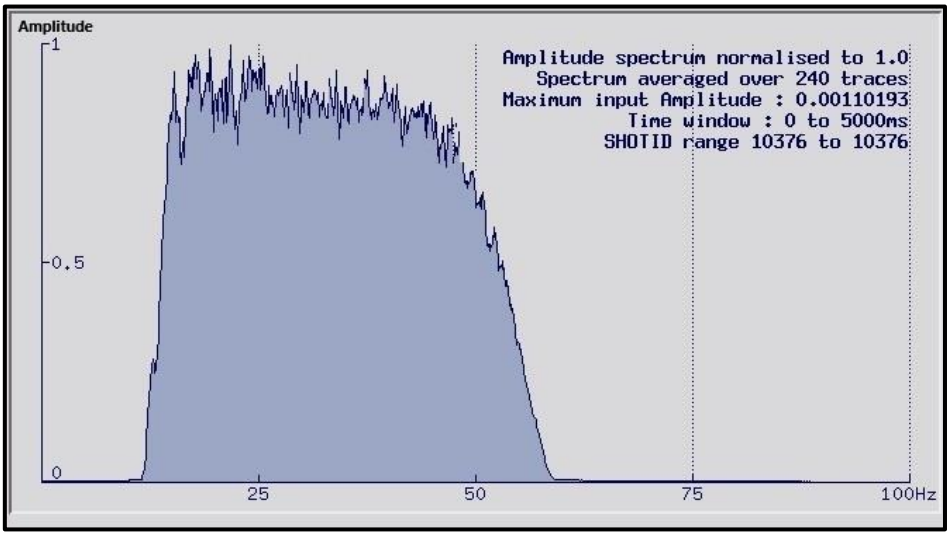

Figure 7: Amplitude spectrum after applying spiking SCDECON, operator length 220 ms, prediction lag 2ms.

3.2 Gapped Surface-Consistent Deconvolution

This kind of deconvolution needs to provide the parameters of operator length, prediction lag, and the whiting noise percentage. Using the software "SCDECON," six tests were applied. The parameters used, operator lengths ranged from 180 ms to 360 ms, the prediction lag ranged from 12 ms to 42 ms, and the fixed whiting noise percentage 0.01% according to (Table-2) to determine the best prediction lag and operator length, as shown in auto-correlogram pre-deconvolution (Fig. 1) for raw data. The result is shown in Fig. 5 post-deconvolution and proves the result by using the amplitude spectrum (Fig. 3) before and after deconvolution (Fig. 6). The extracted data from deconvolution is converted from the shot-gather domain to the CDP-gather domain, and the normal-moveout correction is applied to the data to be ready for stacking [24]. A bandpass filter is used to attenuate the noise resulting from deconvolution to extract the final stack for the data [25]. The bandpass frequencies employed are [11-13] Hz for the high-pass filter range and [45-50] Hz for the low-pass filter range.

Table 2: Tests were applied to find the best parameters for gapped deconvolution.

Operator Length (ms)	Prediction Lag (ms)					
	Test 1	**Test 2**	**Test 3**	**Test 4**	**Test 5**	**Test 6**
180	12	16	20	28	36	42
200						
220						
240						
280						
360						

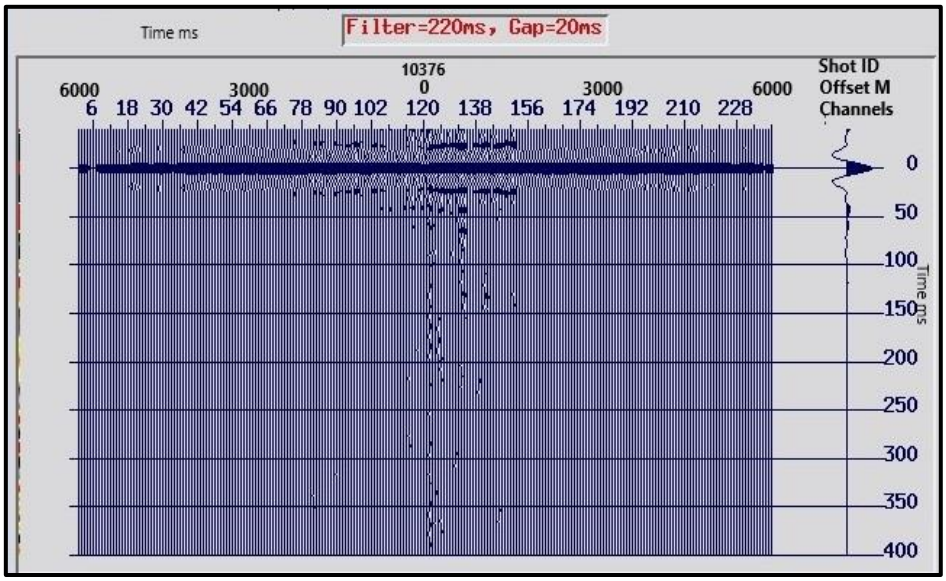

Figure 8: Autocorrelation after applying gapped SCDECON, operator 220 ms, prediction lag 20 ms.

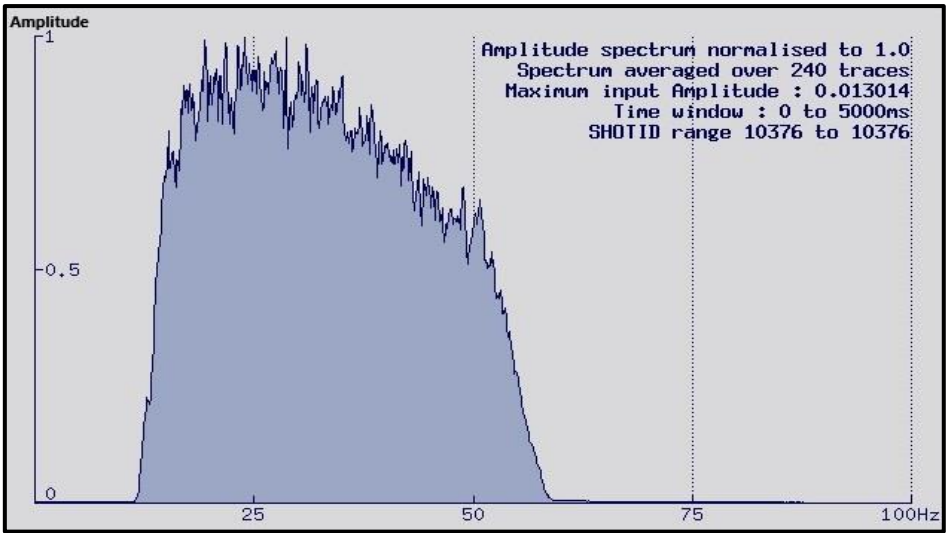

Figure 9: Amplitude spectrum after applying gapped deconvolution, operator 220 ms, prediction lag 20 ms.

4. Results and Discussion

4.1. Spiking SCDECON

The best operator length was found to be 220 ms with a prediction lag of 2 ms and Whiting noise of 0.01% using a comparison between the raw data (Figure-1) and the resultant data from deconvolution (Figure-2). Noise causes small multiples to appear in the autocorrelation [26]. The data could find the effect of spiking on the data by previewing the raw shot-gather in (Figure-7) and matching it with the shot-gather in (Figure-8) after applying spiking surface-consistent deconvolution as shown in yellow and blue ovals.

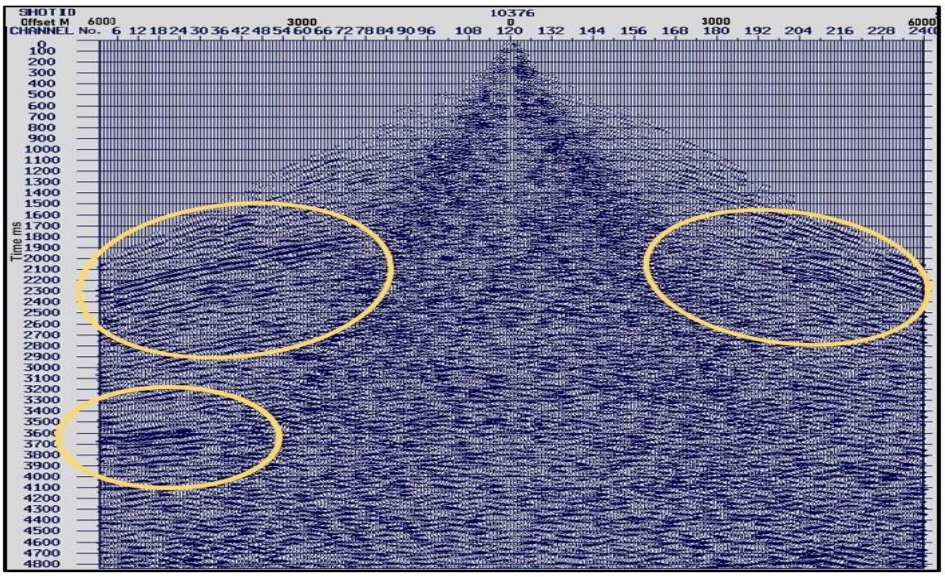

Figure 10: Raw shot-gather

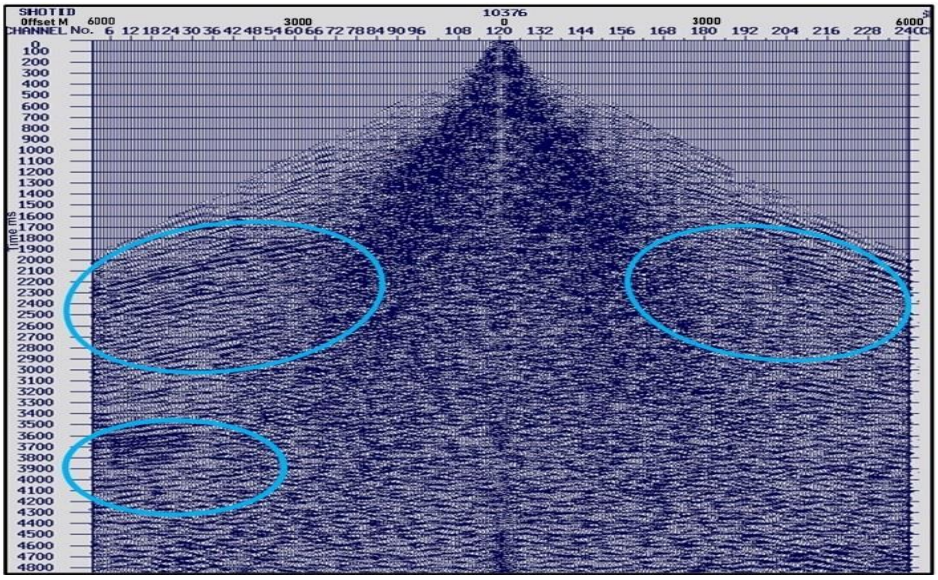

Figure 11: Shot-gather after applying spiking SCDECON, operator length 220 ms, prediction lag 2ms.

Although the data resolution dropped, which represents a disadvantage indicator for this kind of deconvolution, the wavelet continuity in the resulting final stack was better than the raw stack, as shown by the red oval shapes, when compared to the raw stack, as shown in (Figure-9), with the final stack following deconvolution, according to (Figure-10). The black rectangle helps to notice that the noise has vanished from the layers close to the surface to a great degree. In the layer close to the top surface between the time zero and 500 ms, the vertical resolution has become essentially lacking, and some layers have become lighter. This reflects that this deconvolution method is inappropriate for application to enhance the shallow depth wavelets.

In (Figure 10), green arrows indicate the locations of multiple lacking elements. These results suggest that spiking surface-consistent deconvolution is more suitable for noisy seismic data.

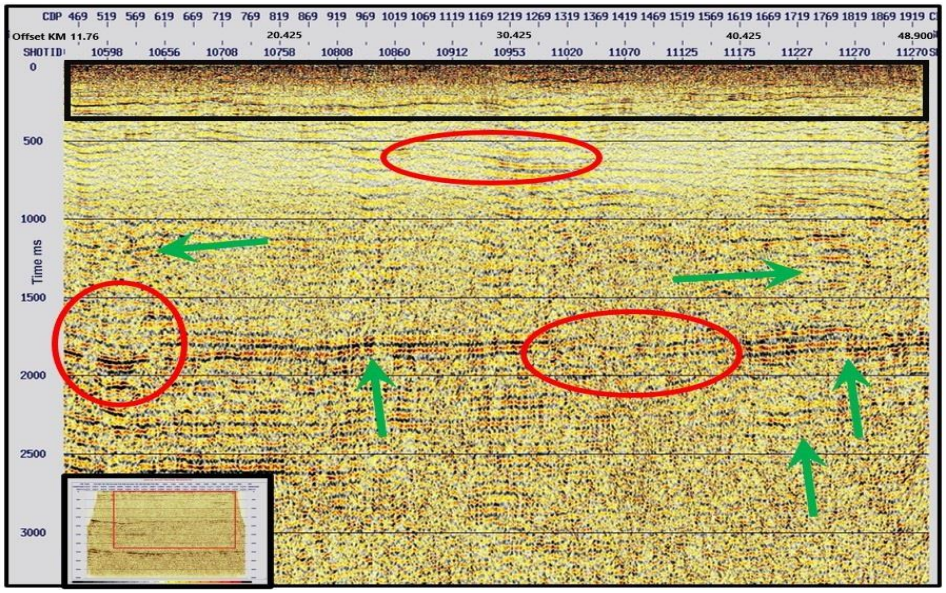

Figure - 12 Raw data stack, the layer near the top surface is noisy, as illustrated by a black rectangle. The red ovals show less continuity of events, and the green arrows refer to the locations of reverberations and the multiples.

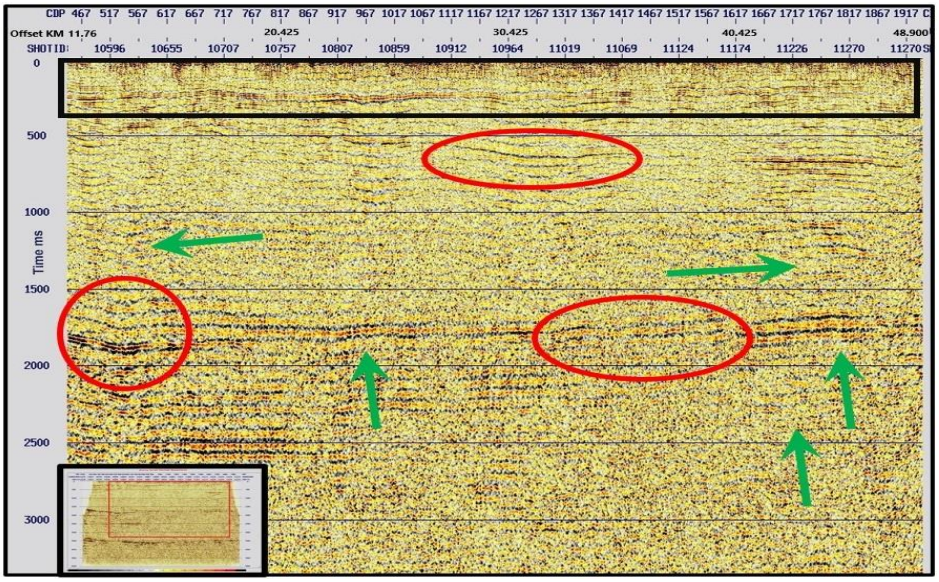

Figure 13: Stack after spiking surface-consistent deconvolution, the operator length was 220 ms, and the prediction lag was 2ms. The area marked with the black rectangle has become less noisy, and the events marked with the red oval have improved and become more continuous. The locations indicated by the green arrows represent areas of improvement, attenuation of multiples, and reverberations.

4.2. Gapped SCDECON

Tests indicate that the best parameters for gapped surface-consistent deconvolution are the operator length of 220 ms, the prediction lag of 20 ms, and the whiting noise of 0.01% percentage. By comparing between the raw autocorrelation Figure 1 with the autocorrelation for the shot-gather following deconvolution Figure 5, these parameters were selected to produce the best autocorrelation devoid of multiples or resonance signals.

By comparing the raw shot-gathers depicted in Figure 11, the impact of the gaps on the data could be investigated using the shot-gather depicted in Figure 12 following Gapped surface-consistent deconvolution.

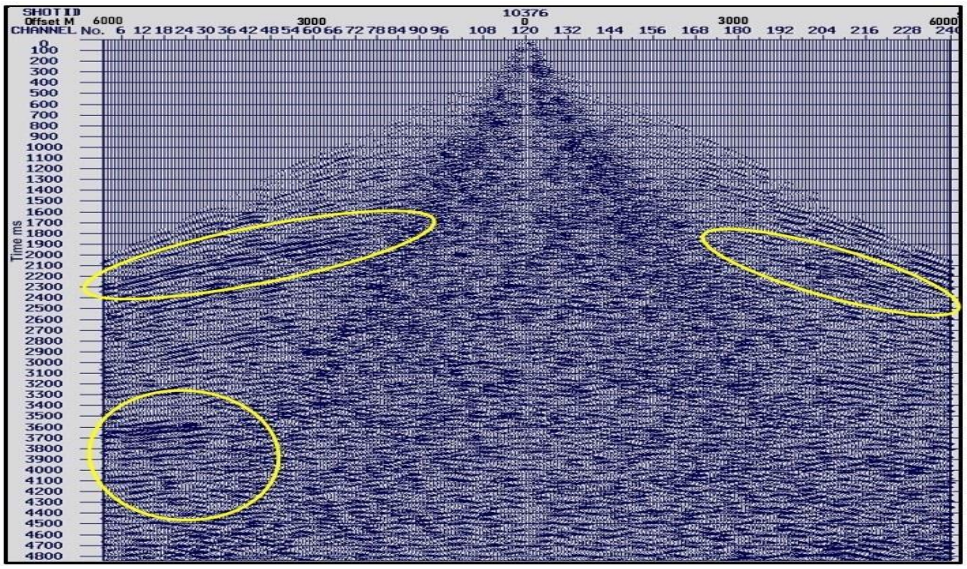

Figure 14: Raw data shot-gather.

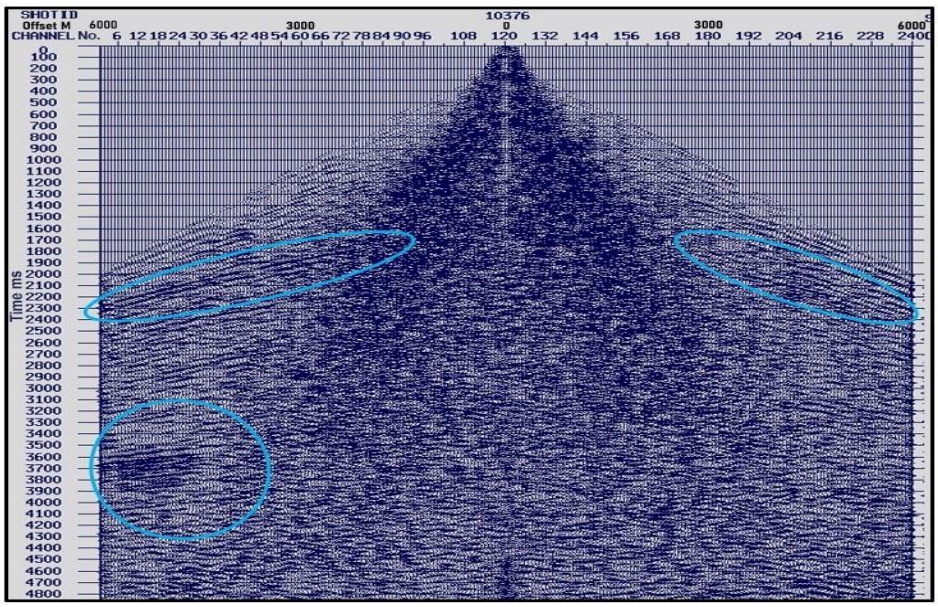

Figure 15: Shot-gather after applying gapped SCDECON, operator 220 ms, prediction lag 20 ms.

Extensive change in stacked data was found after the gapped deconvolution in the surface-consistent method by comparing the raw stack (Figure-13) with the resultant stack after deconvolution (Figure-14), which shows the top part of the stacked data. The unusual discovery was also what was observed in spiking SCDECON, where the events near the surface are clear and can be readily distinguished, as shown in Figure-14 with the red rectangle, but the layers near the surface are almost free of noise that influences the interpretation of the data also some of the events attenuated due to the effect of the deconvolution on attenuation the multiples and reverberations at the shallow depth between zero to 500 ms. The red ovals in the final Figure-14 indicate that the multiples in the data were found to be quite attenuated, hence becoming rather few compared to the previous results in the deconvolution processes. The wavelet distortion in the data virtually disappeared. As the final image by the green arrows indicates, the events have a rather high and clear temporal resolution with high continuity of the wavelets.

For the deep part observations, as shown in Figure-15, raw stack and Figure-16 post-deconvolution stack, the same observations apply to the deep part of the stacked data as to the resultant stack after applying the deconvolution. The events showed significant high attenuation in the multiples, and their continuity was rather clear. Furthermore, distortion was absent from the wavelets.

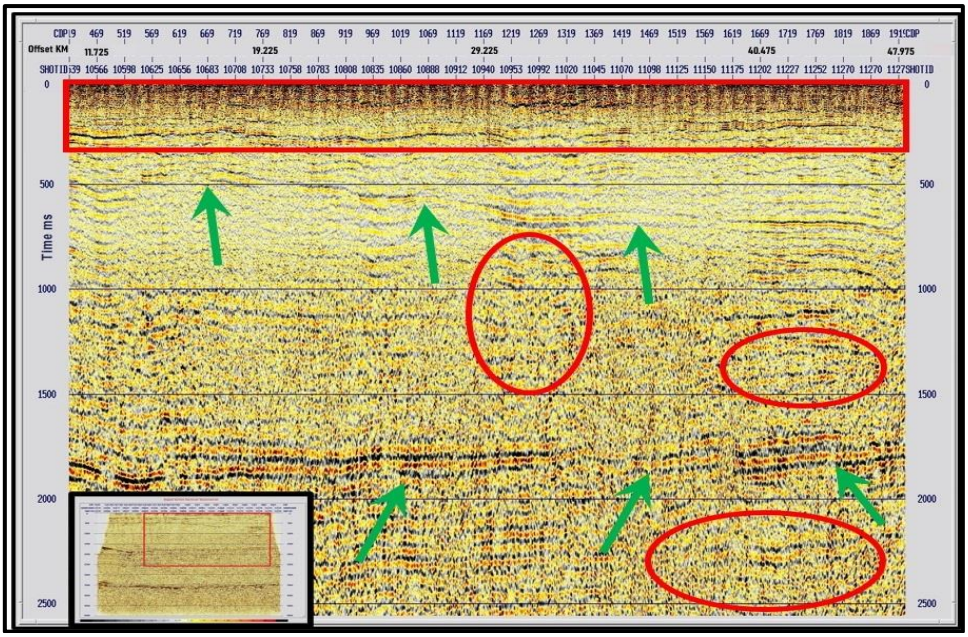

Figure 16: Shallow part of staked raw data. The red rectangle shows the noisy top layers in the shallow part, while the green arrows refer to the events before deconvolution. The red ovals show the locations of multiples and distortion wavelets.

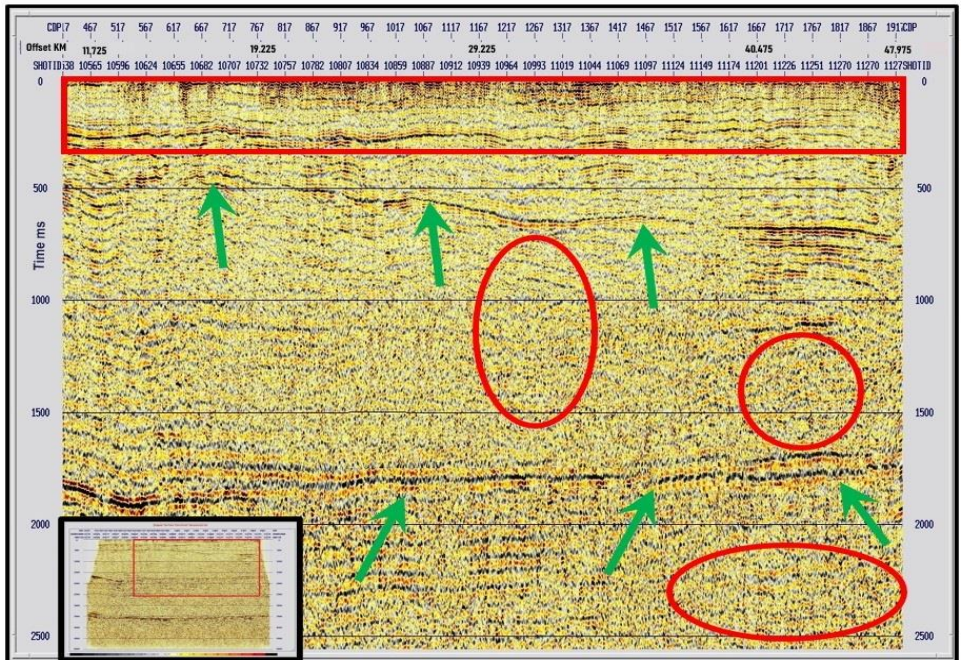

Figure 17: Stack for the shallow data after applying gapped surface-consistent deconvolution, operator 220 ms, prediction lag 20 ms. The red rectangle shows the attenuation of noisy top layers, while the green arrows refer to the events that become sharp. The red ovals show the enchantment in multiples and distortion wavelets.

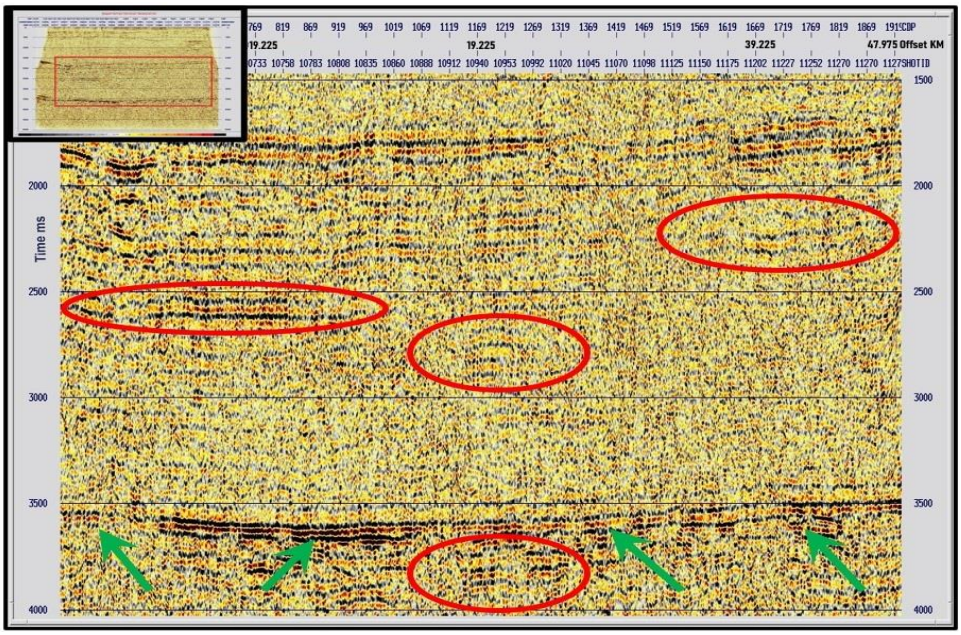

Figure 18: Deep part of staked raw data. The green arrows refer to the events before deconvolution, while the red ovals show the location of multiples and distortion wavelets.

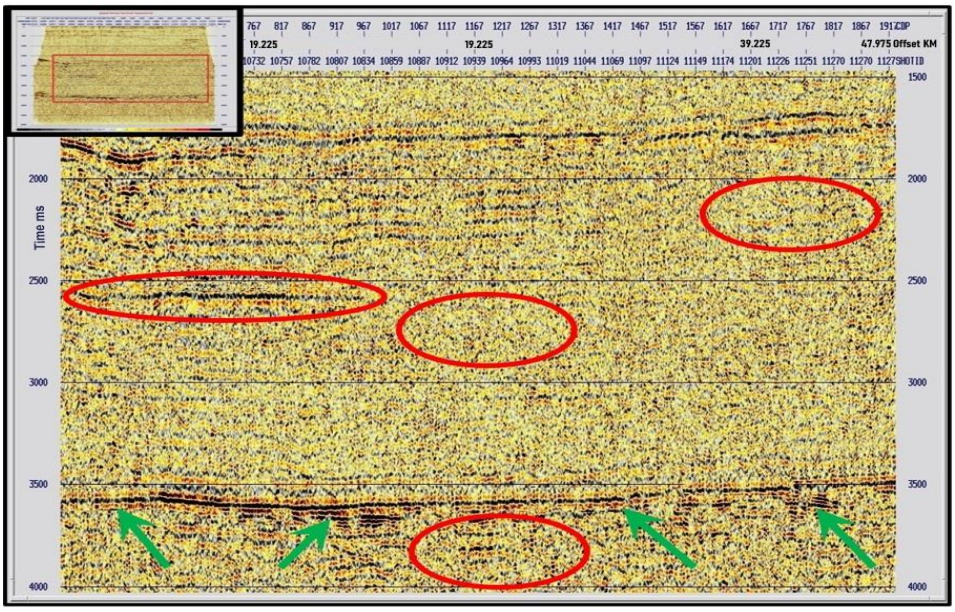

Figure 19: Deep part of staked data after gapped surface-consistent deconvolution, operator 220 ms, prediction lag 20 ms. The green arrows refer to the events that became sharper and clearer, while the red ovals show the attenuation of multiples and distortion wavelets.

5. Conclusions

The test indicates that the best parameters for spiking SCDECON were the operator length of 220 ms, the prediction lag of 2 ms, and the whiting noise of 0.01%, which was proved by using the auto-correlogram, which gave the best result of high correlation to the primary wavelets and free multiplies. Again, this proved the results of the parameters by using the amplitude spectrum graph, which led to making all the bandwidths of the frequencies almost in the same amplitudes. It also made the amplitude spectrum graph like a box shape. After applying the spiking SCDECON to the data, it was found that the effect on the shot-gathers was wide through shrinkage of the primary wavelets. Still, the observation shows less vertical resolution and continuity of the wavelets, especially near the top part. However, there was an

effect on the wavelets on the deep part of the stack, which is considered a disadvantage through using spiking SCDECON. That indicates that the spiking SCDECON is suitable for enhancing seismic data only from mechanical noise.

The best parameters indicated for gapped SCDECON from the tests were the operator length of 220 ms, the prediction lag of 20 ms, and the whiting noise of 0.01%. These parameters were proven using the auto-correlogram technique, which produced the best results concerning the main wavelets and free multiplies. Once more, this demonstrated the effects of the parameters by means of the amplitude spectrum graph, which produced almost identical amplitudes for all the frequencies, rendering the amplitude spectrum like a box form. After applying the deconvolution on the shot gathers, it was vast changes, more than spiking SCDECON by increasing the vertical resolution at the deep part from 3000 ms to the end of the stacked data, and the wavelets became more shrunken, especially at the time 1900 ms, 2500 ms and 3600 ms. Also, the continuity for the primary wavelets gives more stability, especially at 3600 ms. The reverberations, multiples and noise faced high attenuation between zero and 400 ms.

Finally, the gapped SCDECON was found to be the best technique for using the data related to the western region of Iraq, according to the 2D seismic data used in this study.

References

[1] Al Mukhtar, K.S., and Aswad, N.N.: 'Application of the Elevation and Residual Static Correction methods on a selected Seismic data of West Luhais area in the South of Iraq', Iraqi Journal of Science, 2016, pp. 651-662

[2] Bret-Rouzaut, N., and Favennec, J.P.: 'Oil and Gas Exploration and Production: Reserves, Costs, Contracts' (Editions Technip, 2011. 2011)

[3] Ali, A.H., and Al-Rahim, A.M.: 'Linear Noise Removal Using Tau-P Transformation on 3D Seismic Data of Al-Samawah Area-South West of Iraq', Iraqi Journal of Science, 2019, pp. 2664-2671

[4] Kearey, P., Brooks, M., and Hill, I.: 'An introduction to geophysical exploration' (John Wiley & Sons, 400, 2002. 2002)

[5] Ali, K.K., and Khaleefah, L.R.: 'Application of the Surface-consistent DE convolution on a seismic data of Al-Najaf and Al-Muthanna Governorates in the south of Iraq', Iraqi Journal of Science, 2018, pp. 2257-2266

[6] Khalel, R.A., and Al-Rahim, A.M.: 'Structural Interpretations for Zubair Formation in Kumait oil field, Using 3D Seismic Reflection Data, Southern-East Iraq', Iraqi Journal of Science, 2023, pp. 5122-5133

[7] Khorshd, S.Z., and Kareem, R.M.: 'Improve Signal to Noise Ratio (S/N) Using Filters in Field Processing of 3D Seismic Data at Amara Oil field, Southeastern Iraq', Iraqi Journal of Science, 2014, 55, (4A), pp. 1588-1602

[8] Ali, K.K., and Khaleefah, L.R.: 'Application of the Predictive deconvolution on a seismic line Al-Najaf and Al-Muthanna Governorates in Southern Iraq', Iraqi Journal of Science, 2018, pp. 2080-2088

[9] Dondurur, D.: 'Acquisition and processing of marine seismic data' (Elsevier Science. p606, 2018, 1st edn. 2018)

[10] Abdullah, A.M., and Al-Rahim, A.M.: 'Structural interpretation of 2D seismic reflection data of the Khabour Formation in the Upper West Euphrates, western Iraq', Iraqi Journal of Science, 2022, pp. 191-201

[11] Cary, P.W., and Lorentz, G.A.: 'Four-component surface-consistent deconvolution', GEOPHYSICS, 1993, 58, (3), pp. 383-392

[12] Buday, T., and Jassim, S.Z.: 'The Regional Geology of Iraq: Tectonism, Magmatism and Metamorphism' (Geological Survey of Iraq. p445, 1987. 1987)

[13] MDOC: 'Lithological and stratigraphic study for Akkas well-1 (AKK-1)', in Editor (Ed.)^(Eds.): 'Book Lithological and stratigraphic study for Akkas well-1 (AKK-1)' (2023, 1 edn.), pp. 54

[14] Arrowsmith, S.J., Johnson, J.B., Drob, D.P., and Hedlin, M.A.H.: 'THE SEISMOACOUSTIC WAVEFIELD: A NEW PARADIGM IN STUDYING GEOPHYSICAL PHENOMENA', Reviews of Geophysics, 2010, 48, (4)

[15] Li, G., Chen, G., and Zhong, J.: 'Analysis of geophone properties effects for land seismic data', Applied Geophysics, 2009, 6, (1), pp. 93-101

[16] Zihlman, F.N.: 'PLOTSEIS V2.5.3: A DOS Display Program for SEG-Y Formatted Seismic Data' (U.S. Geological Survey, 1995. 1995)

[17] Vossen, R.v., Curtis, A., Laake, A., and Trampert, J.: 'Surface-consistent deconvolution using reciprocity and waveform inversion', Geophysics, 2006, 71, (2), pp. V19-V30

[18] Taner, M., and Coburn, K.: 'Surface-consistent deconvolution: 51st Ann', Internat. Mtg., Soc. Expl. Geophys, 1981

[19] Colombo, D., Rovetta, D., Sandoval-Curiel, E., and Kontakis, A.: 'Transmission-based near-surface deconvolution', GEOPHYSICS, 2020, 85, (2), pp. V169-V181

[20] Schoenberger, M.: 'Optimum weighted stack for multiple suppression', Geophysics, 1996, 61, (3), pp. 891-901

[21] Taner, M.T., and Koehler, F.: 'Surface consistent corrections', Geophysics, 1981, 46, (1), pp. 17-22

[22] Claritas, G.: 'GLOBE Claritas Land 2D Tutorial Version 6.0.', in Editor (Ed.)^(Eds.): 'Book GLOBE Claritas Land 2D Tutorial Version 6.0.' (GNS Science, 2013, edn.), pp.

[23] Yoon, B., Moon, S., Cho, Y., Park, K.-G., and Pyun, S.: 'Frequency-domain autocorrelation imaging condition for 3D elastic time-reversal imaging', Geophysical Prospecting, 2024, 72, (2), pp. 538-549

[24] Kumar, K.: '2D and 3D Land Seismic Data Acquisition and Seismic Data Processing', Andhra University, Andhra Pradesh, India 2005

[25] Bednar, J.B.: 'Applications of median filtering to deconvolution, pulse estimation, and statistical editing of seismic data', Society of Exploration Geophysicists, 1983, 48, (12), pp. 1598-1610

[26] Kumar, D., and Ahmed, I.: 'Seismic Noise', in Gupta, H.K. (Ed.): 'Encyclopedia of Solid Earth Geophysics' (Springer International Publishing, 2020), pp. 1-6